Heliyon 10 (2024) e37298

Contents lists available at ScienceDirect

Heliyon

journal homepage: www.cell.com/heliyon

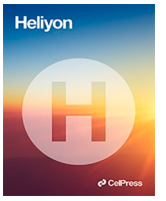

Research article

Theoretical insights into a turn-on fluorescence probe based on naphthalimide for peroxynitrite detection

He Huang, Zhongfu Zou, Yongjin Peng *

College of Modern Industry of Health Management, Jinzhou Medical University, Jinzhou, 121001, PR China

ARTICLE INFO

Keywords:
Reactive oxygen species
Peroxynitrite
Fluorescent probe
Quantum chemistry calculation

ABSTRACT

Compared with other reactive oxygen species, peroxynitrite ($ONOO^-$) has diversified reactions and transformations in organisms, and its specific action mechanism is not very clear. The study of reactive oxygen species is of great significance in the field of physiology and pathology. Recently an effective on/off fluorescent probe HCA-OH was designed by Liu et al. through tethering p-aminophenol to 1,8-naphthalimide directly. The probe HCA-OH could release the fluorophore HCA-NH_2 with good photostability and high fluorescence quantum yield under oxidation of $ONOO^-$ via dearylation process. In this work, the sensing mechanism and spectrum character of probe HCA-OH were studied in detail under quantum chemistry calculation. The electronic structures, reaction sites and fluorescent properties of the probe were theoretically analyzed to benefit us for in-depth understanding the principle of detection on reactive oxygen species ($ONOO^-$) with the fluorescent probe HCA-OH. These theoretical results could inspire the medical research community to design and synthesize highly efficient fluorescent probe for reactive oxygen species detection.

1. Introduction

As a class of highly active molecules, reactive oxygen species exist widely in nature and living organisms, including hydrogen peroxide, singlet oxygen, hypochlorite, peroxynitrite, hydroxyl radical, superoxide anion radical, etc. [1,2] Among them, hydroxyl radical, hypochlorite and peroxynitrite are highly reactive and can destroy most biomolecules [3–7]. In severe cases, they can cause cytopathic changes and death, thus leading to disease and senescence in living organisms. In recent years, more and more experts have paid attention to the biological effects of reactive oxygen species (ROS) in the organism [8–10].

Peroxynitrite ($ONOO^-$) acts as an important organism reactive oxygen species (ROS), which is produced by diffusion control reactions between nitric oxide and superoxide in the biological body [11]. The $ONOO^-$ within the normal concentration range has positive effect on cell function, such as signal transduction, REDOX homeostasis and immune response [12–14]. Once the concentration is too high, $ONOO^-$ can attack lipids, nucleic acids, proteins and many other key biomolecules through oxidation or nitrification, resulting in oxidative damage to cells and tissues. In addition, studies have shown that abnormal production of peroxynitrite can lead to the occurrence and development of many diseases, such as inflammation, cardiovascular disease, neurodegenerative diseases, stroke and cancer [15–23]. Under physiological conditions, $ONOO^-$ has a short life span (10 ms) [24] and is difficult to be directly measured in biological samples. Therefore, it is of important research significance to monitor the intracellular $ONOO^-$ content

* Corresponding author
E-mail address: pengyj@jzmu.edu.cn (Y. Peng).

https://doi.org/10.1016/j.heliyon.2024.e37298
Received 25 August 2023; Received in revised form 28 August 2024; Accepted 30 August 2024
Available online 2 September 2024

changes in real time.

So far, many analytical methods have been used for $ONOO^-$ detection, such as UV–Vis spectroscopy, electron spin resonance, electrochemical analysis, immunohistochemistry and fluorescence [25–34]. In contrast, fluorescence is considered to be a very effective method because of its advantages of non-invasion, high selectivity, fast response and hyperspatial imaging. In recent years, analysts have constructed many $ONOO^-$ fluorescent probes using the $ONOO^-$ induced specific functional group transformation strategy, such as: $ONOO^-$ induced unsaturated double bond breaking, diphenyl phosphonate ester hydrolysis, borate and N-methyl p-hydroxyaniline oxidation etc. [35–45] Although some achievements have been made on the detection and image of the $ONOO^-$ in vivo, there are still some problems in the reported fluorescent probe such as low stokes shift which lead to be susceptible to interferences of its own excitation light and self-absorption fluorescence. Therefore, there is still an urgent need for a simple, fast response with a larger stokes shift $ONOO^-$ fluorescent detection probe.

Through tethering p-aminophenol to 1,8-naphthalimide directly, Liu et al. designed an effective on/off fluorescent probe HCA-OH (Fig. 1) [46]. The probe HCA-OH could release the fluorophore HCA-NH_2 with good photostability and high fluorescence quantum yield under oxidation of $ONOO^-$ via deacylation process. In this work, the sensing mechanism and spectrum character of probe HCA-OH were studied in detail under quantum chemistry method. The electronic structures, reaction sites and fluorescent properties of the probe were theoretically analyzed to benefit us for in-depth understanding the principle of detection on reactive oxygen species ($ONOO^-$) with the fluorescent probe HCA-OH. These theoretical results could inspire the medical research community to design and synthesize highly efficient fluorescent probe for reactive oxygen species detection.

2. Method

The combination of CAM-B3LYP/def2-TZVPD was used to search the stable ground state geometric structures of HCA-OH and HCA-NH_2 with D3 dispersion and GCP correction to remove artificial overbinding effects from BSSE through ORCA 5.0.1 program [47–54]. The reliability of the stable geometric structure searching results was confirmed by non-imaginary frequency found in the vibrational analysis on the probes. Under CAM-B3LYP/def2-TZVPD combination the TDDFT method was used to analyze the excited states of the probes so as the electron excitation and fluorescent properties. This functional and basis set combination CAM-B3LYP/def2-TZVPD were confirmed to be appropriate for studying the excited states of the single organic molecules [55–58]. Multiwfn 3.8(dev) code [59] and VMD 1.9.3 software [60] were used to do the corresponding analyses and delineate the figures respectively.

3. Results

The p-aminophenol moiety in probe HCA-OH was oxidant-sensitive which could be showed by dual descriptor and electrostatic potential (ESP) surface of the probe as shown in Figs. 2 and 3 respectively. The restored fluorescence of HCA-NH_2 could indicate the concentration level of $ONOO^-$ in vivo or in vitro.

The free probe HCA-OH was found to be non-fluorescent in experiment. Upon oxidation of $ONOO^-$ the sensing product HCA-NH_2 was released which led to an obviously fluorescent enhancement at 548 nm. The maxima wavelength of absorption spectrum varied from 460 nm to 431 nm which resulted in a big stokes shift benefiting for the fluorescence detection [46]. The linear correlation between fluorescence intensity of HCA-NH_2 and concentration level of $ONOO^-$ in solution indicated the good potential usage of the fluorescent probe HCA-OH on $ONOO^-$ detection. The density of electron states (DOS) of probe HCA-OH (Fig. 4) and HCA-NH_2 (Fig. 5) clearly showed the energy gap between HOMO and LUMO of HCA-NH_2 was bigger than that of probe HCA-OH which was consistent with the experiment results of the absorption spectrum of the probes. As shown in Figs. 4 and 5, the alkane part (C_4H_9) in probe HCA-OH and HCA-NH_2 has almost no contribution to the HOMO and LUMO of the probes. The HOMO and LUMO of HCA-NH_2 were both contributed form the amino-naphthalimide part which also indicated local excitation character in its optical excitation process and corresponding strong fluorescence. Whereas the HOMO of HCA-OH has the contribution from the amino-naphthalimide and

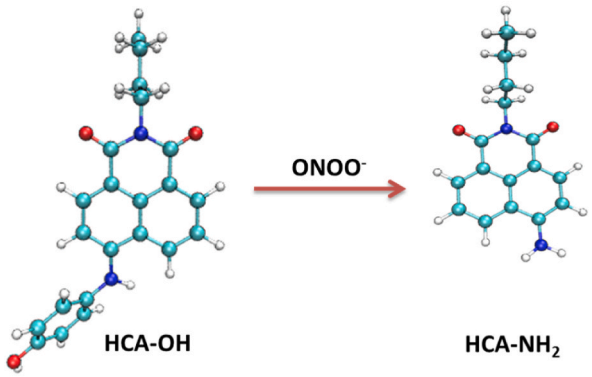

Fig. 1. Structure and mechanism of HCA-OH ($C_{22}H_{20}N_2O_3$) for detecting $ONOO^-$. (sensing product HCA-NH_2, $C_{16}H_{16}N_2O_2$, cyan:C, white:O, blue: N, red:O).

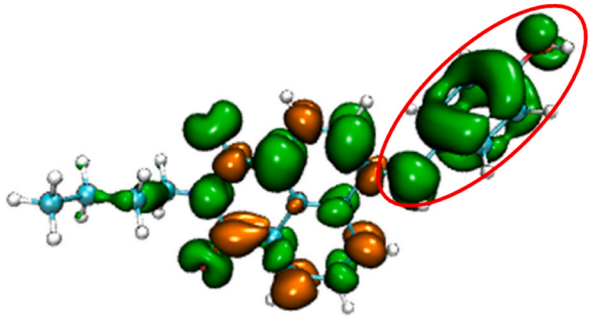

Fig. 2. Dual descriptor of HCA-OH, the big green isovalue map in the red circle indicated the electrophilic reactivity of the p-aminophenol moiety in the probe.

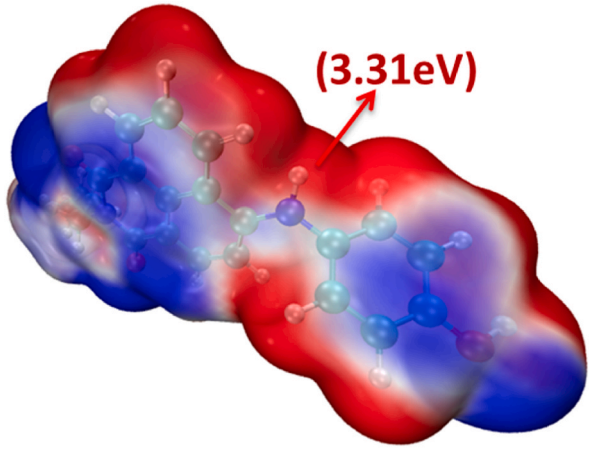

Fig. 3. ESP of HCA-OH, the max value shown in the figure indicated the reactive site in the probe molecule.

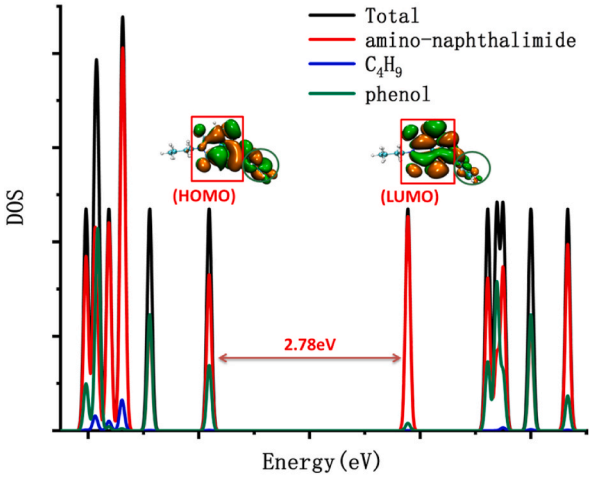

Fig. 4. DOS of HCA-OH

phenol parts simultaneously indicated the charge transfer process in the optical excitation of this probe.

To better understand the electron excitation process in the probe HCA-OH and HCA-NH_2, the structure and electron density variation between the ground state S_0 and first excited state S_1 of the probes were studied through ORCA and multiwfn program under quantum mechanical approach method. From Fig. 6 it can be clearly shown that obvious turn of the phenol plane corresponding to the amino-naphthalimide plane between the stable S_0 and S_1 of the HCA-OH which maybe led to the negligible oscillation strength

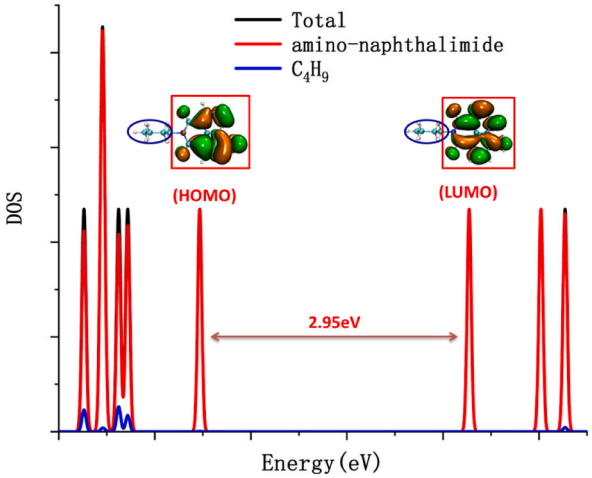

Fig. 5. DOS of HCA-NH_2.

between these two energy states and corresponding fluorescence of the probe. However for HCA-NH_2 as shown in Fig. 7, the structure difference between the stable S_0 and S_1 was hardly to tell which indicated the local exciton characteristic and strong oscillation strength between these two energy states and corresponding fluorescence of this probe. The detail of theoretical electron excitation and emission processes and experimental fluorescence of the two molecules were summarized in Table S1.

From the hole-electron distribution analysis in the electron excitation from S_0 to S_1 in the probe HCA-OH and sensing product HCA-NH_2, the different characteristic of electron transfer in these two molecules were clearly illustrated. It could be clearly showed in Figs. 8 and 9 respectively that electron localized in the amino-naphthalimide part of HCA-NH_2 participated in the excitation process from S_0 to S_1 whereas the electron transfer between amino-naphthalimide part and phenol part of HCA-OH occurred in the excitation process from S_0 to S_1 of the probe.

The contribution of each atom in the S_0 to S_1 process of the probes was clearly shown in atom-atom heat map (Figs. 10 and 11 for HCA-OH and HCA-NH_2 respectively). Number 2 (C atom) in the HCA-NH_2 and number 30 (N atom) in HCA-OH made the biggest contribution to the hole distribution in the corresponding electron excitation process in the probes. (the number of atoms in these two probes could be referenced to Figure S_1 and Figure S_2) The local excitations in the amino-naphthalimide part of HCA-NH_2 and electron transfer from phenol part to amino-naphthalimide part in HCA-OH were also clearly shown in the atom-atom electron transfer heat map of these two probes.

The directional UV–Vis absorption spectrum of the probes could indicate the energy absorbance in the molecule along different directions. Due to the mainly 2D planar structure in HCA-NH_2 it could be deduced that the energy absorbance along the 2D molecular plane should occupy the most part of the UV–Vis absorption spectrum just as shown in Fig. 12, the simulated directional UV–Vis absorption spectrum of the probe. In probe HCA-OH, the deflection between the plane of phenol and amino-naphthalimide led to non-2D planar structure of it. It could be clearly seen in Fig. 13 that the absorption spectrum part along the direction perpendicular to the plane of amino-naphthalimide could not be neglected. The detail analysis of optical excitation and emission process within probe HCA-OH and sensing product HCA-NH_2 were summarized in Tables 1 and 2 respectively. These processes combined the DOS and hole-electron distribution analysis between ground and excited states of probe could explain the luminescence mechanism of the corresponding compounds.

To better understand the structure variation between the ground state S_0 and first excited state S_1, the reorganization energy between two states of the probe HCA-NH_2 and HCA-OH were analyzed and delineated in Figs. 14 and 15 respectively. The deflection of the phenol part in the probe HCA-OH from S_0 to S_1 was resulted in bigger reorganization energy in the excitation process compared with the probe HCA-NH_2 which had a nearly negligible change of structure within the excitation process. In probe HCA-OH the stretching vibration mode located in the phenol part made the biggest contribution to the reorganization energy which was corresponding to the obvious deflection of this part during the excitation process. Whereas in probe HCA-NH_2 the vibration located in the amino-naphthalimide and C_4H_9 parts both had the non-neglected contribution to the reorganization energy in the excitation process which was related with the no obvious structural variation between the stable S_0 and S_1 states of the probe.

4. Conclusions

The sensing mechanism of the single organic molecule fluorescent probe HCA-OH, which was a naphthalimide-based turn-on fluorescence probe for peroxynitrite detection and imaging in living cells, were studied thoroughly under quantum mechanical methods. The dual descriptor and ESP of the probe HCA-OH both indicated the response sites to $ONOO^-$ was the phenol part in the probe molecule. The electronic structures' difference between the probe HCA-OH and HCA-NH_2 was the origin for their different fluorescent characters which led to the applicable for the sensing of $ONOO^-$ through fluorescence detection. All these theoretical

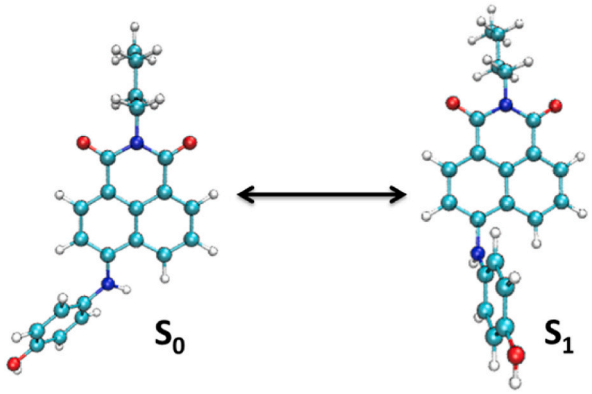

Fig. 6. Stable S_0 and S_1 structure of the HCA-OH.

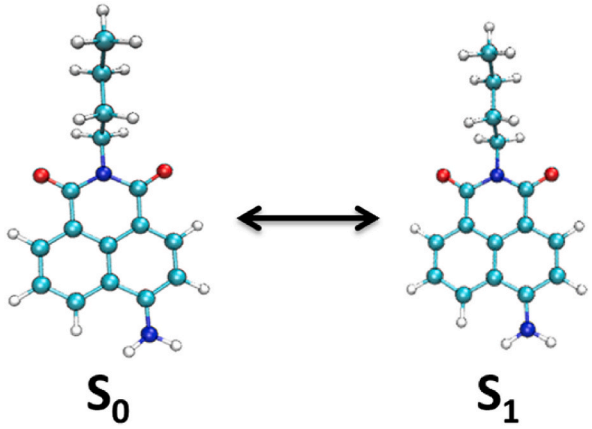

Fig. 7. Stable S_0 and S_1 structure of the HCA-NH_2.

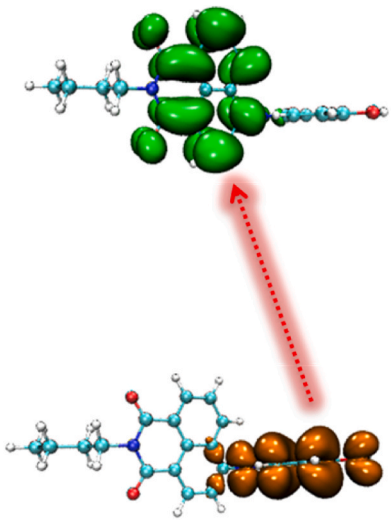

Fig. 8. Electron excitation path from S_0 to S_1 of the HCA-OH, orange and green represented the hole and electron distribution respectively.

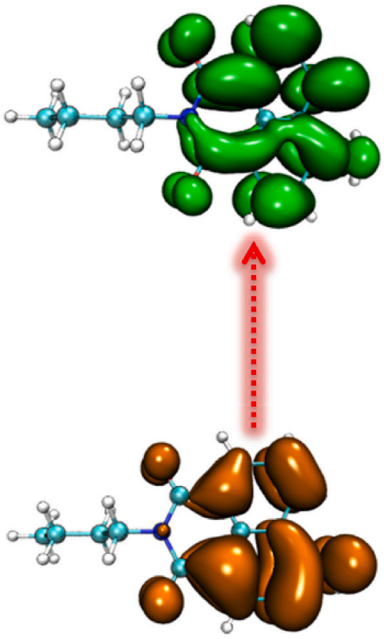

Fig. 9. Electron excitation path from S_0 to S_1 of the HCA-NH_2, orange and green represented the hole and electron distribution respectively.

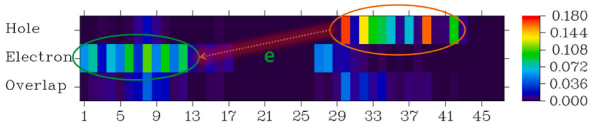

Fig. 10. Atom-atom electron transfer heat map from S_0 to S_1 of the HCA-OH.

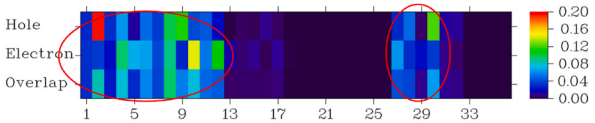

Fig. 11. Atom-atom electron transfer heat map from S_0 to S_1 of the HCA-NH_2.

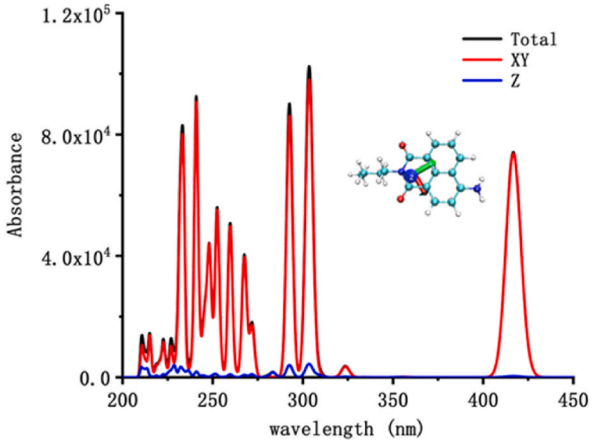

Fig. 12. Simulated directional UV–Vis spectrum of HCA-NH_2.

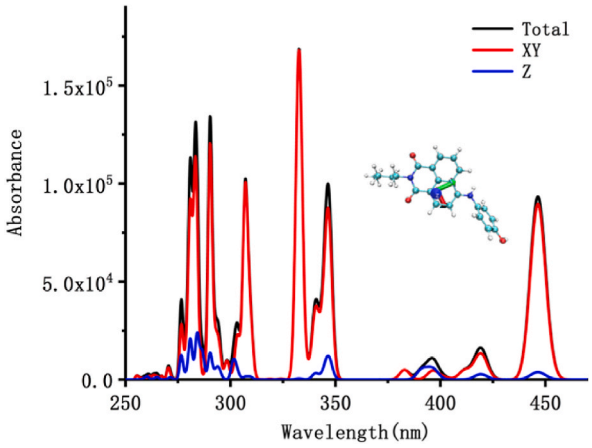

Fig. 13. Simulated directional UV–Vis spectrum of HCA-OH.

Table 1
The main electron excitation processes in HCA-OH and HCA-NH_2.

Compound	Electronic transition[a]	Excitation Energy (nm)	Oscillator strength	Composition[b]	CI[c]
HCA-OH	$S_0 \rightarrow S_1$	**445**	**0.6154**	H → L	**0.7056**
HCA-NH_2	$S_0 \rightarrow S_1$	420	0.9024	H → L	0.7124

[a] Only the excited states with oscillator strength larger than 0.1 were considered.
[b] H stand for HOMO and L stands for LUMO.
[c] Coefficient of the wave function for each excitation was in absolute value.

Table 2
The main electron emission processes in HCA-OH and HCA-NH_2.

Compound	Electronic transition[a]	Emission Energy (nm)	Oscillator strength	Composition[b]	CI[c]
HCA-OH	$S_1 \rightarrow S_0$	**526**	**0.0127**	H → L	**0.7025**
HCA-NH_2	$S_1 \rightarrow S_0$	507	0.8875	H → L	0.7810

[a] b,c same indication as in Table 1.

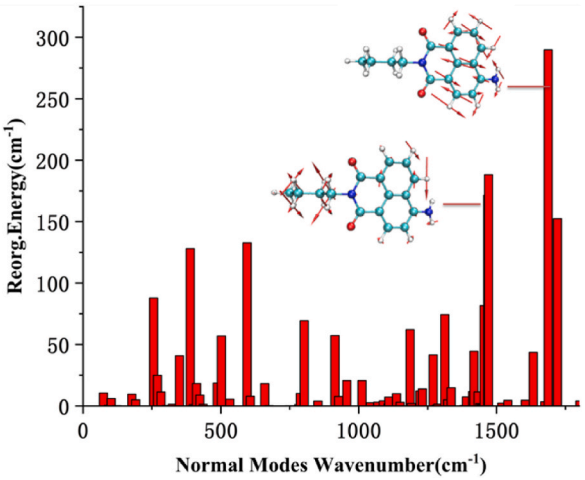

Fig. 14. Reorganization energy between S_0 and S_1 of HCA-NH_2.

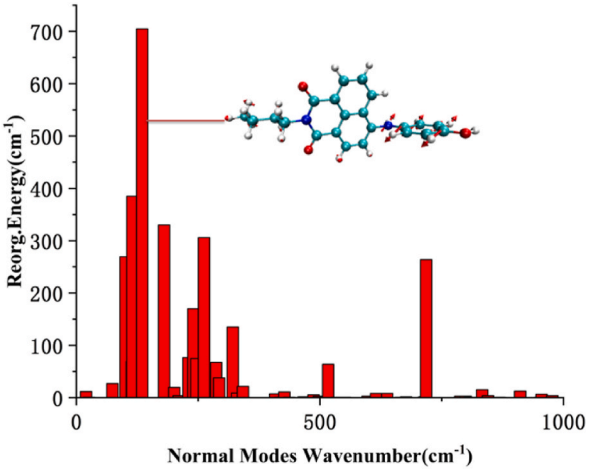

Fig. 15. Reorganization energy between S_0 and S_1 of HCA-OH.

results could provide the insight for designing new efficient functional fluorescent probe for biomarker detection and imaging.

Funding

Natural Science Foundation of Liaoning Province (2022-MS-389, 20180550512, JYTQN201923).

Data availability statement

The original contributions presented in the study are included in the article/supplementary material, further inquiries can be directed to the corresponding author.

CRediT authorship contribution statement

He Huang: Software, Investigation, Data curation. **Zhongfu Zou:** Data curation, Formal analysis. **Yongjin Peng:** Conceptualization, Formal analysis, Funding acquisition, Investigation.

Declaration of competing interest

We have no financial relationships with other groups.

Appendix A. Supplementary data

Supplementary data to this article can be found online at https://doi.org/10.1016/j.heliyon.2024.e37298.

References

[1] B.M. Sahoo, B.K. Banik, P. Borah, A. Jain, Anti Cancer Agents Med. Chem. 22 (2022) 215.
[2] Z. Yu, Q. Li, J. Wang, Y. Yu, Y. Wang, Q. Zhou, P. Li, Nanoscale Res. Lett. 15 (2020).
[3] T.S. Leyane, S.W. Jere, N.N. Houreld, Int. J. Mol. Sci. 23 (2022).
[4] B. Niu, K. Liao, Y. Zhou, T. Wen, G. Quan, X. Pan, C. Wu, Biomaterials 277 (2021) 5471.
[5] M. Kamran, A. Parveen, S. Ahmar, Z. Malik, S. Hussain, M.S. Chattha, M.H. Saleem, M. Adil, P. Heidari, J.-T. Chen, Int. J. Mol. Sci. 21 (2020).
[6] T.M. Bauer, E. Murphy, Circ. Res. 126 (2020) 280.
[7] U.S. Srinivas, B.W.Q. Tan, B.A. Vellayappan, A.D. Jeyasekharan, Redox Biol. 25 (2019).
[8] B. Zhang, C. Pan, C. Feng, C. Yan, Y. Yu, Z. Chen, C. Guo, X. Wang, Redox Rep. 27 (2022) 45.
[9] R. Mittler, S.I. Zandalinas, Y. Fichman, F. Van Breusegem, Nat. Rev. Mol. Cell Biol. 23 (2022) 663.
[10] C.H. Foyer, G. Hanke, Plant J. 111 (2022) 642.
[11] H. Sies, V.V. Belousov, N.S. Chandel, M.J. Davies, D.P. Jones, G.E. Mann, M.P. Murphy, M. Yamamoto, C. Winterbourn, Nat. Rev. Mol. Cell Biol. 23 (2022) 499.
[12] P. Guerby, O. Tasta, A. Swiader, F. Pont, E. Bujold, O. Parant, C. Vayssiere, R. Salvayre, A. Negre-Salvayre, Redox Biol. 40 (2021).
[13] K.K. Griendling, L.L. Camargo, F.J. Rios, R. Alves-Lopes, A.C. Montezano, R.M. Touyz, Circ. Res. 128 (2021) 993.
[14] I.S. Harris, G.M. DeNicola, Trends Cell Biol. 30 (2020) 440.
[15] N. Robinson, R. Ganesan, C. Hegedus, K. Kovacs, T.A. Kufer, L. Virag, Redox Biol. 26 (2019) 101239.
[16] P. Picon-Pages, J. Garcia-Buendia, F.J. Munoz, Biochimica Et Biophysica Acta-Molecular Basis Of Disease 1865 (2019) 1949.

[17] J.A. Bolduc, J.A. Collins, R.F. Loeser, Free Radical Biol. Med. 132 (2019) 73.
[18] R. Radi, Proc. Natl. Acad. Sci. U.S.A. 115 (2018) 5839.
[19] G. Ferrer-Sueta, N. Campolo, M. Trujillo, S. Bartesaghi, S. Carballa, N. Romero, B. Alvarez, R. Radi, Chem. Rev. 118 (2018) 462.
[20] P.A. Campochiaro, T.A. Mir, Prog. Retin. Eye Res. 62 (2018) 24.
[21] S. Bartesaghi, R. Radi, Redox Biol. 14 (2018) 618.
[22] L. Mueller, C. Caris-Veyrat, G. Lowe, V. Boehm, Crit. Rev. Food Sci. Nutr. 56 (2016) 1868.
[23] K. Du, A. Ramachandran, H. Jaeschke, Redox Biol. 10 (2016) 148.
[24] G. Ferrer-Sueta, R. Radi, ACS Chem. Biol. 4 (2009) 161.
[25] Z. Mao, J. Xiong, P. Wang, J. An, F. Zhang, Z. Liu, J.S. Kim, Coord. Chem. Rev. 454 (2022) 214356.
[26] J. Hu, Y. Sun, A.A. Aryee, L. Qu, K. Zhang, Z. Li, Anal. Chim. Acta 1209 (2022) 338885.
[27] N. Kwon, D. Kim, K.M.K. Swamy, J. Yoon, Coord. Chem. Rev. 427 (2021) 213581.
[28] D. Cheng, W. Xu, X. Gong, L. Yuan, X.-B. Zhang, Acc. Chem. Res. 54 (2021) 403.
[29] L. Wu, C. Huang, B.P. Emery, A.C. Sedgwick, S.D. Bull, X.-P. He, H. Tian, J. Yoon, J.L. Sessler, T.D. James, Chem. Soc. Rev. 49 (2020) 5110.
[30] J.-T. Hou, K.-K. Yu, K. Sunwoo, W.Y. Kim, S. Koo, J. Wang, W.X. Ren, S. Wang, X.-Q. Yu, J.S. Kim, Chem 6 (2020) 832.
[31] L. Wu, A.C. Sedgwick, X. Sun, S.D. Bull, X.-P. He, T.D. James, Acc. Chem. Res. 52 (2019) 2582.
[32] T.D. Ashton, K.A. Jolliffe, F.M. Pfeffer, Chem. Soc. Rev. 44 (2015) 4547.
[33] C.C. Winterbourn, Biochim. Biophys. Acta Gen. Subj. 1840 (2014) 730.
[34] S.I. Dikalov, D.G. Harrison, Antioxidants Redox Signal. 20 (2014) 372.
[35] W. Xu, Q. Yang, J. Zeng, L. Tan, L. Zhou, L. Peng, Y. Zhou, C. Xie, K. Luo, Z. Zhang, Sensor. Actuator. B Chem. 359 (2022) 131565.
[36] J. Li, R. He, S. Duan, J. Li, X. Han, Y. Ye, Chin. J. Org. Chem. 42 (2022) 2428.
[37] X. Ji, J. Zhou, C. Liu, J. Zhang, X. Dong, F. Zhang, W. Zhao, Anal. Methods 14 (2022) 5027.
[38] Y. Huang, L. Yu, L. Fu, J. Hou, L. Wang, M. Sun, X. Wang, L. Chen, Sensor. Actuator. B Chem. 370 (2022) 132410.
[39] L. He, H. Liu, J. Wu, Z. Cheng, F. Yu, Chem.–Asian J. 17 (2022) e202200388.
[40] J. Gu, Y. Liu, J. Shen, Y. Cao, L. Zhang, Y.-D. Lu, B.-Z. Wang, H.-L. Zhu, Talanta 244 (2022) 123401.
[41] Y.-X. Ye, X.-Y. Chen, Y.-W. Yu, Q. Zhang, X.-W. Wei, Z.-C. Wang, B.-Z. Wang, Q.-C. Jiao, H.-L. Zhu, Analyst 146 (2021) 6556.
[42] F. Xin, J. Zhao, W. Shu, X. Zhang, X. Luo, Y. Tian, M. Xing, H. Wang, Y. Peng, Y. Tian, Analyst 146 (2021) 7627.
[43] M. Wang, C. Wang, W. Song, W. Zhong, T. Sun, J. Zhu, J. Wang, Spectrochim. Acta Mol. Biomol. Spectrosc. 251 (2021) 119398.
[44] Y. Shen, L. Dai, Y. Zhang, H. Li, Y. Chen, C. Zhang, Spectrochim. Acta Mol. Biomol. Spectrosc. 228 (2020) 117762.
[45] L. Wu, X. Tian, H.-H. Han, J. Wang, R.R. Groleau, P. Tosuwan, B. Wannalerse, A.C. Sedgwick, S.D. Bull, X.-P. He, T.D. James, Chemistryopen 8 (2019) 1407.
[46] X. Liu, F. Gu, X. Zhou, W. Zhou, S. Zhang, L. Cui, T. Guo, RSC Adv. 10 (2020) 38281.
[47] P. Liu, Y.-l. Liu, H. Huang, G. Bai, Y.-j. Peng, Spectrochim. Acta Mol. Biomol. Spectrosc. 289 (2023).
[48] X.Y. Lin, S.H. Sun, Y.T. Liu, Q.Q. Shi, J.J. Lv, Y.J. Peng, Front. Chem. 10 (2023) 990979.
[49] Y.-l. Liu, H. Huang, Y.-j. Peng, J. Mol. Struct. 1255 (2022) 132441.
[50] F. Neese, Wiley Interdiplinary Reviews Computational Molecular Ence, vol. 8, 2018, p. e1327.
[51] M. de Wergifosse, S. Grimme, J. Chem. Phys. 150 (2019) 094112.
[52] E. Caldeweyher, S. Ehlert, A. Hansen, H. Neugebauer, S. Spicher, C. Bannwarth, S. Grimme, J. Chem. Phys. 150 (2019) 154122.
[53] L. Goerigk, S. Grimme, Wiley Interdiscip. Rev.-Comput. Mol. Sci. 4 (2014) 576.
[54] S. Grimme, S. Ehrlich, L. Goerigk, J. Comput. Chem. 32 (2011) 1456.
[55] B. Komjati, A. Urai, S. Hosztafi, J. Koekoesi, B. Kovats, J. Nagy, P. Horvath, Spectrochim. Acta Mol. Biomol. Spectrosc. 155 (2016) 95.
[56] M.T.P. Beerepoot, D.H. Friese, N.H. List, J. Kongsted, K. Ruud, Phys. Chem. Chem. Phys. 17 (2015) 19306.
[57] K. Okuno, Y. Shigeta, R. Kishi, H. Miyasaka, M. Nakano, Journal Of Photochemistry And Photobiology a-Chemistry 235 (2012) 29.
[58] P.J. Aittala, O. Cramariuc, T.I. Hukka, Chem. Phys. Lett. 501 (2011) 226.
[59] T. Lu, F. Chen, J. Comput. Chem. 33 (2012) 580.
[60] W. Humphrey, A. Dalke, K.K. Schulten, J. Mol. Graph. 14 (1995) 33.